Invited Paper

Why is THz Sensitive to Protein Functional States? Oxidation State of Cytochrome C

Yunfen He [1], J.-Y. Chen [2], J. R. Knab [3], Wenjun Zheng [1] and A. G. Markelz [1*]
[1] Physics Department, University at Buffalo, SUNY, Buffalo, NY 14260
[2] Washington State University, Pullman, WA
[3] Technical Univeristy of Delft, Delft, Netherlands
[*1] E-mail: amarkelz@acsu.buffalo.edu

（Received July 02, 2010）

Abstract: We investigate the presence of structural collective motions on a picosecond time scale for the heme protein, cytochrome c, as a function of oxidation and hydration, using terahertz (THz) time-domain spectroscopy and molecular dynamics simulations. Structural collective mode frequencies have been calculated to lie in this frequency range, and the density of states can be considered a measure of flexibility. A dramatic increase in the THz response occurs with oxidation, with the largest increase for lowest hydrations and highest frequencies. For both oxidation states the measured THz response rapidly increases with hydration saturating above ~25% (g H_2O/g protein), in contrast to the rapid turn-on in dynamics observed at this hydration level for other proteins. Quasi-harmonic collective vibrational modes and dipole-dipole correlation functions are calculated from the molecular dynamics trajectories. The collective mode density of states alone reproduces the measured hydration dependence providing strong evidence of the existence of these collective motions. The large oxidation dependence is reproduced only by the dipole-dipole correlation function, indicating the contrast arises from diffusive motions consistent with structural changes occurring in the vicinity of a buried internal water molecule.

Keywords: Structural collective motions, Terahertz, Molecular dynamics, Heme protein, Cytochrome c

doi: 10.11906/TST.149-162.2010.12.15

1. Introduction

Protein function relies on structural dynamics, with time scales ranging from picoseconds to beyond seconds. The key to understanding protein interactions is the understanding of dynamics and coupling of motions associated with the dynamics. The transitions to the different configurations involved in function are routinely reproduced by trajectories involving only the first few structural collective modes, suggesting the importance of these modes in understanding and tailoring of protein interactions. However, there is some debate as to whether large scale structural collective motions exist and if instead dynamics are entirely directed Brownian motion. Such uncorrelated diffusive motion would need to serendipitously access the proper configuration for reactions to go forward. Concerted motions could explain the observed high physiological on-rates and affinities [1-4]. Recent neutron spin echo and X-ray inelastic scattering have seemed to verify that collective motions do occur [5,6], however these measurements did not address if these motions are dependent on environment of functional state. Generally knowledge of coupled motion is limited by the requirement of crystallizing the sample at key points in the dynamic pathway, capturing static snapshots, then using computational modeling to study the dynamics and conformational changes that take place between the structural snapshots. Even when we have crystallographic evidence of motion that reveals the extent and direction of gross or small conformational fluctuations, we cannot determine if the motions are in fact interdependent. While

these measurements map correlations they cannot discern if the motions of individual atoms are actually coupled. This question is critical in the quest for tailoring allosteric interactions.

Computational studies of collective motions have used three types of analysis: normal modes, quasiharmonic modes and course grain modes. An intuitive example of large-scale collective motion is the hinging motion of lysozyme. The hinge motion is immediately apparent as the upper and lower portions of the protein clamp down upon the substrate resulting in more effective cleavage. However one can also visualize the molecule without substrate and the hinge continuously oscillating. This motion was first calculated over 20 years ago by Karplus and Brooks for lysozyme, with a hinge bending resonant frequency of 3.6 cm^{-1} = 0.108 *THz* [7]. There is some skepticism if these harmonic motions occur in vivo and normal mode analysis, based on the minimized energy structure at zero temperature, is not an accurate model of biological systems. Nevertheless the motions predicted by normal modes and principal component analysis lead to root mean squared displacements in good agreement with experimental results [8,9]. The calculated time scales for these correlated motions can be from the ps to ns.

To fully map out these motions requires an experimental tool which can both resolve energy and momentum transfer in the picosecond range. Inelastic neutron scattering (INS) is such a technique, however its application is limited since it is not a table top instrument and requires large samples (~100 *mg*) and deuteration. Another relevant spectral technique is terahertz time domain spectroscopy (THz TDS). Previously we and others have used terahertz time domain spectroscopy to measure the dielectric function of protein samples which has contributions from vibrational and diffusive motions in the protein and adjacent solvent:

$$\varepsilon(\omega) = \varepsilon_o + \int \frac{f(\omega')g(\omega')}{(\omega'^2 - \omega^2) + i\gamma(\omega')\omega} d\omega' + \varepsilon_r \int_0^\infty \frac{h(\tau)d\tau}{1 + i\omega\tau} \qquad (1)$$

where ε_o is the DC dielectric constant. The second term on the right hand side contains the vibrational density of states (VDOS) $g(\omega)$, oscillator strength $f(\omega)$ and damping coefficient $\gamma(\omega)$. The third term is the relaxational response, assuming Debye relaxation for a distribution of relaxation times $h(\tau)$. Typically, what is measured is the absorption coefficient $\alpha(\omega)$ and the refractive index $n(\omega)$. Relating these measured quantities to the vibrational and relaxational response, one obtains:

$$\alpha_{vib}(\omega) = \int \frac{g(\omega')f(\omega')\omega\gamma(\omega')}{(\omega'^2 - \omega^2)^2 + \gamma(\omega')^2\omega^2} d\omega' \quad \text{and} \quad \alpha_{relax}(\omega)n_{relax}(\omega) = \int \frac{1}{c}\frac{h(\tau)\tau\omega^2}{1-\tau^2\omega^2} d\tau \qquad (2)$$

where $\alpha_{vib}(\omega)$ is the absorption coefficient which arises from the vibrational motions and $\alpha_{relax}(\omega)n_{relax}(\omega)$ is the product of the absorption coefficient and refractive index arising from the relaxational response. The relaxational response is always a broad absorbance. For small systems (5-20 atoms), the frequency dependence of the vibrational and relaxational responses are distinct, with the vibrational resonances widely spaced and relatively narrow. For large macromolecules, the collective vibrational modes become dense and individual modes begin to overlap. The spectrum becomes sufficiently dense that it is difficult to distinguish the structural vibrational response from localized side chain relaxational rotations [10]. Such a distinction is important for applications such as allosteric inhibitor design, where the binding of the inhibitor is constructed

to interfere with the structural motions necessary for function [11]. This strategy will fail if there is not sufficient coupling of motions. Our ability to characterize structural motions distinct from diffusive ones is challenged by the similarity in the relaxational and vibrational response for large macromolecules. However the manner in which these different types of motions change with environment or functional state can be distinct. To test for the presence and contribution of picosecond collective vibrational modes, we compare systematic measurements of cytochrome c (CytC) as a function of hydration and oxidation with the calculated response from the collective vibrational motions and the dipole-dipole correlation function which includes relaxational response. We find collective vibrational motions account for the hydration dependence observed in the THz dielectric response. However, the frequency dependence appears to be dominated by the relaxational motions of water and side chains. Furthermore the large oxidation dependence observed is only reproduced when relaxational motions are included.

CytC is an ideal system to test the role of collective motions, as it has already been shown to have a significant contrast in the terahertz dielectric response as a function of oxidation[12]. We can thus compare calculations of the oxidation dependence with these measurements in order to establish which motions reproduce the results. CytC is a protein of increasing interest as its multiple functions become revealed. The primary role of CytC is to participate in the metabolism process in the mitchondria through the transfer of an electron from cytochrome c reductase to cytochrome c oxidase, both embedded in the inner mitochondrial membrane. Recently, it has become clear that CytC plays an important role in apoptosis, both within the mitchondria and during its release into the cytosol[13]. Furthermore, CytC is an excellent model heme protein to consider fundamental questions of protein dynamics, as it is sufficiently small for systematic comparisons to theoretical modeling.

The physiochemical properties of CytC can be explained in terms of the differences in the dynamic behavior of the two redox states. Eden and co-workers proposed that the oxidized form of CytC is more flexible than the reduced form [14], based on an estimated 40% increase in the apparent compressibility of CytC upon oxidation. This was interpreted by the authors as an increase in the root mean squared volume fluctuations. However, it is difficult to rigorously separate the properties of the protein from that of the solvent in compressibility measurements. For instance Kharakoz et al. found that the increase in apparent compressibility is only 2% upon CytC oxidation [15]. X-ray diffraction measurements appeared to give some support to higher flexibility in the ferri state, as the atomic mean squared displacement (msd) as measured by the Debye Waller factor increases for ferri over ferro[16]. The motions contributing to msd can be both collective as in structural vibrational modes and local as in side chain librations. A quantitative relationship can be drawn between the collective modes and the structural flexibility using the frequency dependence of the vibrational density of states (VDOS). In particular the contribution of collective modes to msd can be associated with the VDOS in comparison to the thermal energy. Low frequency modes below k_BT are thermally occupied and these motions will contribute to the msd, whereas high frequency modes with energies on the order of k_BT or higher have lower occupation and these motions would have a smaller contribution to the msd. Thus a protein with a large VDOS at low frequencies is more flexible than one with the VDOS shifted to higher frequencies.

The X-ray and compressibility results suggest that the flexibility is higher in the ferri state and thus one might expect a red shift in the VDOS with oxidation. THz-TDS was previously used to

investigate if the implied changes in the VDOS occurs with the CytC flexibility change with oxidation [12]. A large increase in the THz dielectric response was observed with oxidation consistent with an increase in the low frequency VDOS and a higher flexibility. A number of observations since those studies have suggested caution when directly relating the dielectric response to the VDOS. These include the exploration of the role of local relaxational motions in the THz dielectric response in hydration measurements on lysozyme[17]; nuclear vibrational resonance spectroscopy (NRVS) measurements showing a very slight increase in the VDOS for the modes coupled to the heme Fe with oxidation of CytC[18]; and the report of a large enhancement in the dielectric response for water immediately adjacent to the protein over that of bulk water[19]. This last point is critical in that if the equilibrium water content is dependent on oxidation state, the THz contrast observed may arise from the different water contributions and not from a density of states change. It is therefore important that the comparison between oxidation states be made at equivalent water content. Here we present systematic measurements as a function of measured water content and oxidation state. These measurements confirm the large oxidation dependence in the dielectric response at low hydrations.

More importantly the systematic hydration and oxidation dependence data allows us to test the degree structural vibrational modes contribute to the terahertz response and to determine the origin of the oxidation dependence by comparison with molecular dynamics (MD) simulations.

In order to elucidate the fundamental dynamics that are responsible for the THz dielectric response, we perform MD simulations. We present two simulation approaches, both using calculated molecular trajectories: harmonic vibrational response based on quasiharmonic analysis; and the full response as determined by the power spectrum of the dipole-dipole correlation function. Quasiharmonic analysis is also referred to as principle component analysis (PCA). PCA is essentially a harmonic analysis allowing for changes in the effective force constants at finite temperature. In this method, the MD simulation is utilized to obtain effective modes of vibration from the atomic fluctuations about an average structure. These modes include the anharmonic effects neglected in a normal mode calculation [20]. PCA introduces temperature dependent anharmonicity, but still calculates the harmonic vibrational modes of the system as well as the dipole derivative for each mode, which is used to calculate the absorption coefficient. This analysis does not capture diffusive motion such as librational motion of side chains and individual rotational motion of solvent molecules. To capture the full dielectric response involving all motions one must use the complete trajectory calculated from the full potential. This full dielectric response can be calculated by the power spectrum of the dipole-dipole correlation function. The dipole-dipole correlation function is calculated from the MD trajectories and then the Fourier transform of the correlation function reveals the frequency dependent absorption coefficient. We perform both types of calculations as a function of hydration and oxidation state and compare with the measured results.

The hydration dependence of protein dielectric response over a broad frequency range up to 10 GHz was characterized 40 years ago, where for proteins studied, an abrupt increase in the dielectric response was observed as the hydration increases above 30 g water/100 g protein (30% wt)[21-24]. We find the measured hydration dependence of the picosecond dynamics for both oxidation states of CytC deviates from this rapid increase, and that the VDOS calculated using PCA reproduces the observed hydration dependence. This ability to reproduce the measured hydration dependence with the quasiharmonic modes indicates the presence of collective modes

at THz frequencies. However PCA does not reproduce the observed oxidation dependence, suggesting that anharmonic motions need to be included to fully reproduce the measured response. Consistent with this we find that the calculated dielectric response from the full dipole-dipole correlation function does reproduce the oxidation dependence. We propose that the THz dielectric response is dominated by the anharmonic motions such as surface side chain rotational motions or possibly motion of an internally bound water molecule.

2. Results

We compare the absorption coefficients of ferri-CytC and ferro-CytC films as a function of water content in Fig. 1. The absorption coefficient rapidly increases with hydration for both oxidation states, however the rate of change appears to be dependent on both the frequency and oxidation state. For all frequencies the ferri absorption coefficient initially increases rapidly with a near power law dependence. The rate of increase then abruptly decreases at a cross over point ~ 20-25% wt. In contrast, the ferro-CytC α increases linearly with hydration, but this rate also decreases abruptly at higher hydrations. This cross over behavior from a rapid increase with hydration to a saturation behavior for both oxidation states is readily apparent in the refractive index data in Fig. 2. For both ferri and ferro samples the index rapidly increases at low hydrations and then the hydration dependence abruptly decreases with a cross over point for both oxidation states at ~ 23-25% wt. This dielectric hydration dependence for CytC is different than that seen in other proteins as will be discussed.

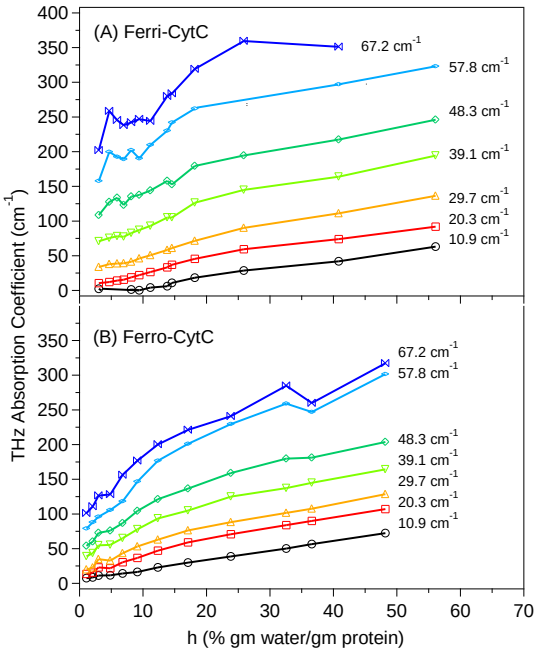

Fig. 1 THz absorption coefficients of Ferri (A) and Ferro (B) CytC at several representative frequencies as a function % hydration.

Comparing the response at equivalent water content we see in Fig. 1 and 2, an obvious oxidation dependence of the picosecond response as was reported earlier. The dependence is most dramatic for the index measurements, where the ferri state values are consistently larger for all

hydrations and frequencies. While the absorption coefficient does increase in the ferri state at higher frequencies and lower hydrations, this contrast decreases with increasing hydration and at lower frequencies. Looking at the 10.9 cm^{-1} data the α values are nearly indistinguishable for ferri and ferro over the entire hydration range, however at a higher frequency such as 48.4 cm^{-1} α at 5% wt has approximate values of 120 cm^{-1} in the ferri state and only 80 cm^{-1} in the ferro state whereas at 9% wt $\alpha \sim 125$ cm^{-1} for the ferri state and 100 cm^{-1} for the ferro state. This oxidation dependence is consistent with Takano and Dickerson's B-factors where the average B-factor was found to increase from 18.7 in the ferro state, to 22.7 in the ferri state [16].

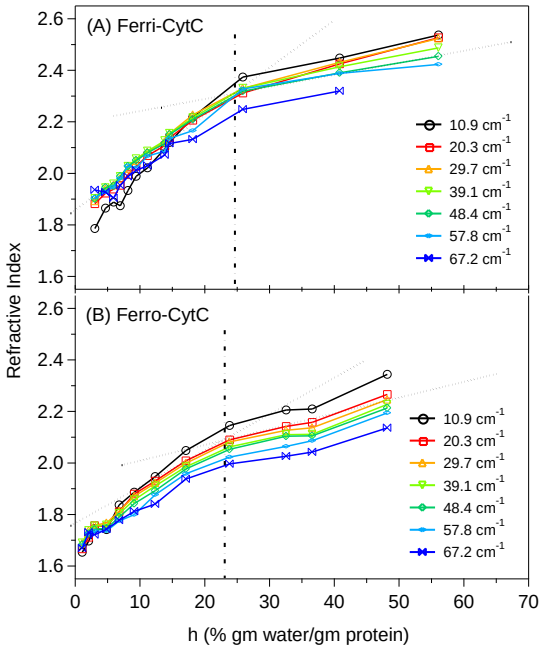

Fig. 2 Refractive indices of Ferri (A) and Ferro (B) CytC at several representative frequencies as a function of % hydration. Lines drawn as guide to the eye.

We now turn to how well the calculated response for only collective modes versus the full response reproduces the measured results. In addition to the quasiharmonic mode analysis that we present here, we performed the simpler normal mode analysis where the force constants are extracted from the curvature of the potential at the minimized energy. However we found no agreement between the calculated normal modes and the measured hydration or oxidation dependence indicating that normal mode analysis is inadequate for accurately describing the dynamics.

As suggested in Eq. 1, the dielectric response is related to both the density of vibrational states and the oscillator strength of each state. In the small field approximation we can calculate this IR absorbance from the dipole derivative of the mode. In the usual approximation this is simply the dipole moment change that occurs with atomic motion along the eigenvector of the mode. It is assumed the partial charges of the individual atoms remains constant as the atoms move along the eigenvector. This partial charge assumption is considered the most problematic of this approach to calculating the IR absorbance. Previously we have suggested that due to the somewhat homogeneous distribution of charge and high asymmetry of protein structures, that the absorption

integrated overall orientations is nearly independent of the mode.

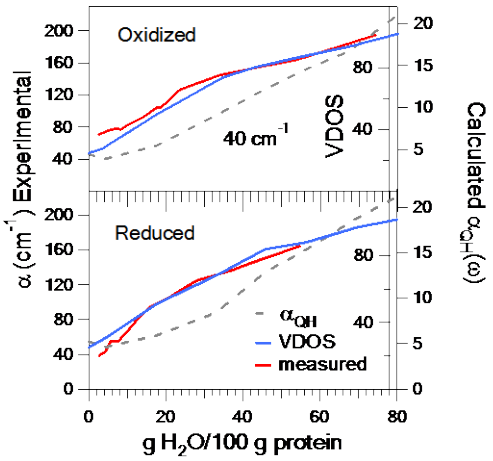

Fig. 3 The hydration dependent measured absorption coefficient, calculated quasiharmonic VDOS, and calculated absorbance α (ω□) for Ferri-CytC and Ferro-CytC at 40 cm^{-1}.

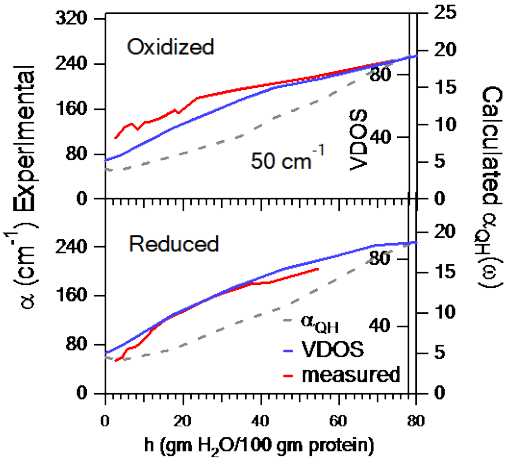

Fig. 4 The hydration dependent meas- ured absorption coefficient, calculated quasiharmonic VDOS, and calculated absorbance α_{QH} (ω□) for Ferri-CytC and Ferro- CytC at 50 cm^{-1}.

Fig. 3 and 4 show comparisons of the hydration dependence of the measured absorbance, the calculated VDOS and the calculated absorbance for both ferri CytC and ferro CytC. Fig. 3 shows the results at 40 cm^{-1} and Fig. 4 shows the results for 50 cm^{-1}. The hydration dependence of the VDOS has excellent agreement with the measured response for both oxidation states. This impressive agreement suggests A) the presence of structural vibrational modes contributing to the dielectric signal and B) these modes are responsible for the observed hydration dependence. The hydration dependence of the calculated absorbance deviates from the measured absorption coefficients. It is possible that this is in part due to the assumption of constant partial charges in the dipole derivative calculations. However, at the lowest hydrations the VDOS deviates from the agreement. For oxidized the low hydration VDOS is lower than the measurements, whereas for reduced the low hydration VDOS is higher than the measurements for both frequencies shown. The VDOS does not reproduce the oxidation dependence. To summarize, the quasiharmonic VDOS has excellent agreement with the measured hydration dependence of the picosecond dielectric response for both oxidation states. The agreement is less good for the calculated

absorbance, and neither VDOS nor the calculated absorbance reproduce the oxidation dependence.

To include local diffusive motions that contribute to the THz dielectric response, we calculated the hydration and oxidation dependent dipole-dipole correlation function. The Fourier transform of this function gives the product of the frequency dependent absorption coefficient and the refractive index, $\alpha(\omega)\, n(\omega)$. As seen in Fig. 2, the measured refractive index has little frequency dependence so we directly compare the calculated $\alpha(\omega)n(\omega)$ with the measured $\alpha(\omega)$.

Fig. 5 compares the calculated frequency dependent $\alpha(\omega)n(\omega)$ for oxidized and reduced CytC at low hydration level (~3.63 % wt for ferri CytC, and ~4.50 % wt for ferro CytC). The calculated response reproduces qualitatively the experimentally observed oxidation dependence. After exhaustive attempts using normal modes and PCA, the oxidation dependence could not be reproduced by any of the harmonic analyses, strongly suggesting that the oxidation dependence is manifest in diffusive motions, not the collective motions.

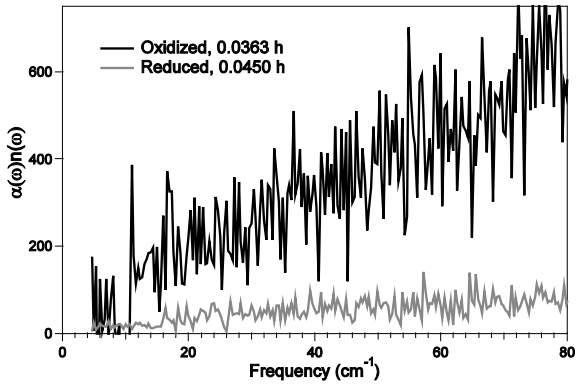

Fig. 5 The frequency dependent $\alpha(\omega)n(\omega)$ (calculated from dipole-dipole correlation) for oxidized CytC and reduced CytC.

3. Discussion

The main result of this work is the demonstration of the relevance of collective modes in the picosecond response. With respect to the origin of the hydration dependence seen in the collective modes at these frequencies we would suggest that at low hydrations the added water adds to the net system, it cannot readily be treated as a separate component and thus the total biomolecular structure increases with the bound water participating in the collective modes. This is very much similar to the picture of the Havenith group [19]. At sufficiently high hydrations, the water is no longer strongly associated with the protein and this additional water contributes as added bulk water.

The quasiharmonic VDOS never captures the low frequency diffusive motions of surface side chains. The residence times for these motions were calculated with typical times ~ 2-10 *ps* [26]. These motions have been discussed by Sokolov and others when analyzing the anharmonicity in the neutron temperature dependence [27] and will be present in the calculated full trajectory. The result that the observed oxidation state dependence is not reproduced by any of the harmonic analysis, but is reproduced by the dipole-dipole correlation indicates that the oxidation

dependence arises from relaxational motions. We suggest that the internal bound water dynamics are influenced by the local electrostatics and it is these motions that give rise to the oxidation dependence seen in the THz response. Even at our lowest hydrations we do not entirely remove the internal water. At low hydrations these few internally bound waters provide a large contribution to the overall signal and therefore an oxidation dependence is observed. At higher hydrations the surface water, mobile surface side chains and the vibrational modes begin to dominate the signal, and the internal water has little net contribution, so the oxidation dependence is very slight at the higher hydrations.

To conclude, terahertz spectroscopy is sensitive to protein environment and functional state. Structural collective modes as calculated by PCA reproduce the measured hydration dependence of absorption coefficient, demonstrating their contribution to the picosecond response. The oxidation dependence of the picosecond response is only reproduced by analysis of the complete trajectory, demonstrating that it is manifest only in the diffusive motions of either the side chains or the internal water. The evidence of structural collective modes in these smaller molecular weight proteins is consistent with recent results using neutron spin echo measurements (NSE) on somewhat more massive proteins[6,30]. The terahertz spectroscopy approach may provide a critical complementary technique to NSE for collective modes on shorter time scales.

4. Materials and Methods

4.1 Sample Preparation and Characterization

Preparation of oxidized and reduced CytC films measured in THz time domain spectroscopy is described in a previous study [12]. Solutions were pipetted onto clean infrasil quartz substrates with half the substrate left bare for referencing. The films were characterized by UV/Vis absorption to verify the oxidation state (see supplementary material). The thickness of the dried films is measured to both verify uniformity and to determine absolute absorption coefficients and refractive indices. Film thicknesses were typically on the order of 100 μm with thickness variation < 5% for a given film. See ref [31] for method of film thickness determination.

4.2 Isotherm Determination

To compare the picosecond dielectric response of ferro and ferri samples at equivalent water content we measured the isotherms for both oxidation states. The water content for a given relative humidity often follows the B.E.T. thermal equati:

$$h(x) = \frac{a h_m x}{(1+x)[1+(a-1)x]} \tag{3}$$

where h(x) is the water content as % wt, that is, g water/100 g protein; a is a parameter representing the potential water absorption capacity of the protein; h_m is a parameter representing the humidity for monolayer of water; and x is the relative pressure of the gas, namely, the relative humidity. See supplementary material for method and results.

4.3 THz TDS

An N_2 purged terahertz time domain spectroscopy system (THz TDS) whose bandwidth is in the range of 5 cm^{-1} and 86 cm^{-1} is used to monitor the change in absorbance and index with oxidation states of CytC films at different hydration. The THz radiation is generated by using a Hertzian dipole antenna and detected electro-optically [33,34]. All measurements were performed at room temperature and under hydration control. Substrates were mounted on a brass holder with two apertures for the reference bare substrate and the CytC film. The plate is mounted in a closed hydration cell with the relative humidity controlled by flushing the cell with a hydrated gas from a Licor dewpoint generator. Nitrogen (air) was used as the flushing gas for the ferro (ferri) films. The closed hydration cell is placed at the focus of the THz TDS system.

We measure the terahertz dielectric response of both oxidized and reduced CytC films as a function of hydration. The time required for CytC films to reach hydration equilibrium is determined by TGA (thermogravimetric analysis) and terahertz transmissions. The time constants determined by TGA are 30 minutes for dehydration and one hour for hydration. The time constants determined from the terahertz transmission data are consistent with those obtained from the TGA data. To ensure equilibrium hydration the samples were exposed to a given relative humidity in the hydration cell for at least one hour for film dehydration and two hours for film hydration. As the substrates were mounted vertically we were limited in our highest hydrations by the film's hydration threshold for flowing. For ferri (ferro) -CytC films, the highest water content achieved was 75 % wt (57 % wt). A transmission measurement consists of toggling between the sample and reference apertures. Because the reference is in the same humidity cell along with the sample, we remove any water absorption due to the atmosphere of the humidity cell. The real part of the refractive index and the absorption coefficient are extracted from the terahertz transmission data in the standard way [35].

4.4 Molecular Dynamics Calculations

Version 32 of the CHARMM program [36] with all-atom parameter set 22 [37] is used. Initial x-ray crystal structure files of CytC are taken from the Protein Data Bank, with entry code 1HRC. Heme group partial charges for ferro and ferri states are taken from reference [38]. The heme group is patched to CytC though axial ligated bounds, Met 80 and His 18 and covalent bounds, Cys14 and Cys17. CytC with different hydrations are simulated by solvating a protein with a layer of water molecules with different thicknesses between 1.5 Å and 7 Å by using the "SOAK" command in Insight II. The structures of the solvated proteins are built in CHARMM by using TIP3 force field. The whole system goes through energy minimization process. The minimized structures are used to do the MD simulation.

The MD simulation was carried out with an integration time step of 0.001 *p*s. The system was heated to 300 *K* with a temperature increment of 100 *K* after each 1000 steps. Temperature equilibration was followed by a constant temperature MD run. The trajectory is 1ns, starting with 399 *ps* equilibrium run, being followed by a 601*ps* production run. We find the water rapidly moves to equilibrium positions with the water structure resembling X-ray measurements within 50 *ps*.

From the production run of the MD simulation the average structure of each protein was determined separately using the corresponding 6001 frames and, superimposing each structure onto the average structure, a quasiharmonic vibrational analysis was performed. This is done by diagonalizing the whole covariance matrix for a given protein. The calculation output includes the eigenvalues (mode frequency), the eigenvectors, and the dipole derivatives for each mode [39].

The integrated intensity □ as defined absorptivity and is proportional to the absorption coefficient for a mode with eigenfrequency ν_k [40]. We draw a distinction of Γ with the often calculated absorption intensity, A. A is defined in the classic textbooks and differs from Γ by a factor of ν_k and is not directly related to the derivation of the absorption coefficient from Fermi's Golden rule. The double harmonic approximation consists of both the calculated the modes from a harmonic expansion of the potential and an approximation of the dipole moment inner product using the quadratic term in the Taylor expansion of the dipole. Γ can be obtained from the dipole derivatives calculated from the quasiharmonic analysis using [41]:

$$\Gamma_k = \frac{N_0 \pi}{3c^2 (4\pi\varepsilon_0)\nu_k} \left(\frac{\partial p}{\partial Q_k}\right)^2 \tag{4}$$

where ε_0 is the permittivity of vacuum, and N_0 is the Avogadro number and the magnitude of the dipole derivative

$$\left(\frac{\partial p}{\partial Q_k}\right)^2 = \left(\frac{\partial p_x}{\partial Q_k}\right)^2 + \left(\frac{\partial p_y}{\partial Q_k}\right)^2 + \left(\frac{\partial p_z}{\partial Q_k}\right)^2 \tag{5}$$

A Lorentzian function $\alpha_{QH}(\nu) = \sum_k \frac{1}{\pi} \frac{\Gamma_k \gamma^2}{(\nu - \nu_k)^2 + \gamma^2}$ is used to calculate the net integrated intensity, proportional to the net absorption coefficient. γ is a parameter specifying the full width at half maximum of a vibrational resonance and is set to $4\,cm^{-1}$.

The absorption coefficient per unit length α(ω) and the refractive index n(ω) are related to the imaginary part of the dielectric constant ε"(ω) by α(ω)n(ω) = (ω/c) ε"(ω). Within linear-response theory, α(ω) n(ω) is given by the power spectrum of the time-correlation function of the total dipole operator [42]:

$$\alpha(\omega)n(\omega) = \frac{2\pi\omega^2\beta}{3cV} \int_{-\infty}^{\infty} dt e^{-i\omega t} < M(0)M(t) >$$

Where M is the total dipole moment of the system, V is the volume of the system, and where $\beta = (k_B T)^{-1}$ is the inverse temperature. We calculate the time dependence of the total dipole moment M(t) for the trajectory assuming constant partial charges for all atoms during the entire trajectory.

Acknowledgements

This work was supported by ARO grant DAAD 19-02-1-0271, ACS grant PRF 39554-AC6, NSF CAREER grant PHY-0349256, NSF REU grant DMR-0243833 and NSF IGERT grant DGE0114330.

References

[1] Goodey, N.M. & Benkovic, S.J. "Allosteric regulation and catalysis emerge via a common route". *Nature Chemical Biology* 4, 474-82, (2008).

[2] Hammes-Schiffer, S. & Benkovic, S.J. "Relating Protein Motion to Catalysis". *Annu. Rev. Biochem.* 75, 519-41, (2006).

[3] Lange, O.F. et al. "Recognition DynamicsUp toMicroseconds Revealed from an RDC-Derived Ubiquitin Ensemble in Solution". *Science* 340, 1471-75, (2008).

[4] Jarymowycz, V.A. & Stone, M.J. "Fast Time Scale Dynamics of Protein Backbones: NMR Relaxation Methods,Applications, and Functional Consequences". *Chem. Rev.* 106, 1624-1671, (2006).

[5] Liu, D. et al. "Studies of Phononlike Low-Energy Excitations of Protein Molecules by Inelastic X-Ray Scattering". *Phys. Rev. Lett.* 101, 135501, (2008).

[6] Biehl, R. et al."Direct Observation of Correlated Interdomain Motion in Alcohol Dehydrogenase". *Phys. Rev. Lett.* 101, 138102, (2008).

[7] Brooks, B. & Karplus, M. "Normal modes for specific motions of macromolecules: Application to the hinge bending mode of lysozyme". *Proceedings of the National Academy of Sciences of the United States of America* 82, 4995-4999, (1985).

[8] Teeter, M.M. & Case, D.A. "Harmonic and Quasiharmonic Descriptions of Crambin". *J. Phys. Chem.* 94, 8091-97, (1990).

[9] Zoete, V., Michielin, O. & Karplus, M. "Relation between Sequence and Structure of HIV-1 Protease Inhibitor Complexes: A Model System for the Analysis of Protein Flexibility". *J. Mol. Biol.* 315, 21-52, (2002).

[10] Markelz, A.G. "Terahertz Dielectric Sensitivity to Biomolecular Structure and Function". *IEEE J. Sel. Topics in Quantum Electronics* 14, 180-190, (2008).

[11] Kern, D. & Zuiderweg, E.R. "The role of dynamics in allosteric regulation". *Current Opinion in Structural Biology* 13, 748–757, (2003).

[12] Chen, J.-Y., Knab, J.R., Cerne, J. & Markelz, A.G. "Large oxidation dependence Observed in Terahertz Dielectric Response for Cytochrome C". *Phys. Rev. E. Rapid* 72, 040901, (2005).

[13] Kagan, V.E. et al. "Mitochondria-targeted disruptors and inhibitors of cytochrome c/cardiolipin peroxidase complexes:A new strategy in anti-apoptotic drug discovery". *Mol. Nutr. Food Res.* 53, 104-114, (2009).

[14] Eden, D., Matthew, J.B., Rosa, J.J. & Richards, F.M. "Increase in Apparent Compressibility of Cytochrome c upon Oxidation". *Proceedings of the National Academy of Sciences of the United States of America* 79, 815-819, (1982).

[15] Kharakoz, D.P. & Mkhitarian, A.G. "Changes in the contractibility of the cytochrome c globule during redox transition". *Mol. Biol.* 20, 396-406, (1986).

[16] Takano, T. & Dickerson, R.E. "Redox Conformation Changes in Refined Tuna Cytochrome c". *Proceedings of the National Academy of Sciences of the United States of America* 77, 6371-6375, (1980).

[17] Knab, J.R., Chen, J.Y., He, Y. & Markelz, A.G. "Terahertz Measurements of Protein Relaxational Dynamics". *Proc. of the IEEE* 95, 1605-10, (2007).

[18] Leu, B.M. et al. Vibrational Dynamics of Iron in Cytochrome c. *J. Phys. Chem. B* 113, 2193–2200, (2009).

[19] Ebbinghaus, S. et al. "An extended dynamical hydration shell around proteins". *Proc. Natl. Acad Sci. U.S.A.* 104, 20749–20752, (2007).

[20] Balog, E. et al. "Direct Determination of Vibrational Density of States Change on Ligand Binding to a Protein". *Phys. Rev. Lett.* 93, 28103, (2004).

[21] Pethig, R. *Dielectric and electronic properties of biological materials*, Wiley, New York, (1979).

[22] Bone, S. & Pethig, R. "Dielectric Studies of the Binding of Water to Lysozyme". *Journal of Molecular Biology* 157, 571-575, (1982).

[23] Bone, S. & Pethig, R. "Dielectric Studies of Protein Hydration and Hydration-induced Flexibility". *Journal of Molecular Biology* 181, 323-326, (1985).

[24] Rupley, J.A. & Careri, G. "Protein Hydration and Function". *Adv. Protein Chem.* 41, 37-172, (1991).

[25] Pethig, R. Ch. 4. in *Protein Solvent Interactions* (ed. Gregory, R.B.) 265, Dekker Inc., New York, (1995).

[26] Best, R.B., Clarke, J. & Karplus, M. "What Contributions to Protein Side-chain Dynamics are Probed by NMR Experiments? A Molecular Dynamics Simulation Analysis." *J. Mol. Biol.* 349, 185-203, (2005).

[27] Roh, J.H. et al. "Onsets of Anharmonicity in Protein Dynamics". *Phys. Rev. Lett.* 95, 038101, (2005).

[28] Achterhold, K. et al. "Vibrational dynamics of myoglobin determined by the phonon-assisted Mo¨ssbauer effect". *Phys. Rev. E* 65, 051916, (2002).

[29] Leu, B.M. et al. "Resilience of the Iron Environment in Heme Proteins". *Biophysical Journal* 95, 5874–5889, (2008).

[30] Bu, Z., Biehl, R., Monkenbusch, M., Richter, D. & Callaway, D.J.E. "Coupled protein domain motion in Taq polymerase revealed by neutron spin-echo spectroscopy". *Proc Natl Acad Sci U S A.* 102, 17646–17651, (2005).

[31] Whitmire, S.E. et al. "Protein Flexibility and Conformational State: A comparison of collective vibrational modes of WT and D96N bacteriorhodopsin". *Biophys. J.* 85, 1269-1277, (2003).

[32] Gascoyne, P.R.C. & Pethig, R. "Experimental and theoretical aspects of hydration isotherms for biomolecules". *J. Chem. Soc. Faraday Trans.* 73, 171-180, (1977).

[33] Grischkowsky, D. & Katzenellenbogen, N. "Femtosecond Pulses of Terahertz Radiation: Physics and Applications". in *OSA Proceedings on picosecond electronics and optoelectronics*, Vol. 9 (eds. Sollner, T.C.L. & Shah, J.) OSA, Washington, DC, (1991).

[34] Jiang, Z. & Zhang, X.-C. "Terahertz Imaging via Electrooptic Effect". *IEEE Transactions on Microwave Theory and Techniques* 47, 2644-2650, (1999).

[35] Knab, J., Chen, J.-Y. & Markelz, A. "Hydration Dependence of Conformational Dielectric Relaxation of Lysozyme". *Biophys. J.* 90, 2576-2581, (2006).

[36] Brooks, B.R. et al. "CHARMM: a program for macromolecular energy, minimization, and dynamics calculations". *J. Comput. Chem.* 4, 187-217, (1983).

[37] MacKerell, A.D., Jr. et al. "All-atom empirical potential for molecular modeling and dynamics studies of proteins". *J. Phys. Chem. B* 102, 3586-3616, (1998).

[38] Autenrieth, F., Tajkhorshid, E., Baudry, J. & Luthey-Schulten, Z. "Classical Force Field Parameters for the Heme Prosthetic Group of Cytochrome c". *Journal of Computational Chemistry* 25, 1613-1622, (2004).

[39] Levy, R.M., Rojas, O.d.l.L. & Friesner, R.A. "Quasi-Harmonic Method for Calculating Vibrational Spectra from Classical Simulations on Multidimensional Anharmonic Potential Surfaces". *J. Phys. Chem.* 88, 4233-4238, (1984).

[40] Person, W.B. & Zerbi, G. *Vibrational Intensities in Infrared and Raman Spectroscopy*, Elsevier Scientific Publishing, (1982).

[41] Galabov, B.S. & Dudev, T. *Vibrational Intensities*, Elsevier Science, Amsterdam, (1996).

[42] McQuarrie, D.A. *Statistical Mechanics.* First edn, University Science Books, Sausalito, CA, (2000).